G-Fall: Device-free and Training-free Fall Detection with Geophones

Yandao Huang*, Wenqiang Chen*, Hongjie Chen, Lu Wang, and Kaishun Wu†

College of Computer Science and Software Engineering, Shenzhen University, China
†PCL Research Center of Networks and Communications, Peng Cheng Laboratory, Shenzhen, China
{chenwenqiang2016, huangyandao, chenhongjie2016}@email.szu.edu.cn, {wanglu, wu}@szu.edu.cn

Abstract—The inevitable aging trend of the world's population brings a lot of challenges to the health care for the elderly. For example, it is difficult to guarantee timely rescue for a single-resided elder who falls at home. Under this circumstance, a reliable automatic fall detection machine is in great need for emergent rescue. However, the state-of-the-art fall detection systems are suffering from serious privacy concerns, having a high false alarm or being cumbersome for users. In this paper, we propose a device-free fall detection system, namely G-Fall, based on geophones. We first decompose the falling mode and characterize it with time-dependent floor vibration features. By leveraging Hidden Markov Model (HMM), our system is able to recognize the fall event precisely and achieve training-free recognition. It requires no training from the elderly but only an HMM template learned in advance through a small number of training samples. To reduce the false alarm rate, we propose a novel reconfirmation mechanism, namely Energy-of-Arrival (EoA) positioning to assist in recognizing a human's fall. Extensive experiments have been conducted on 12 human subjects. The results demonstrate that G-Fall achieves a 95.74% recognition precision with a false alarm rate of 5.30% on average. Furthermore, with the assistance of EoA, the false alarm rate is reduced to nearly 0%.

Index Terms—Fall detection, floor vibration, geophone, device-free, training-free

I. INTRODUCTION

Worldwide, there were more than 960 million people aged over 60 years in 2017. By 2050, that number is projected to be more than double its size in 2017, hitting to around 2.1 billion [1]. For the seniors, fall is one of the most prevalent problems that they have to face daily. According to the World Health Organization, approximately 28-35% of adults aged 65 and older fall each year, increasing to 32-42% for those who aged over 70 [2]. The hazard of non-fatal falls commonly includes bruises, internal bleeding, and bone fractures. When it comes to a fatal one, the fall event will be the symbol of a man's death. Among all the fall injury events, about 60% of them happen at home [3], which means that there are a large number of elders who live alone cannot get medical treatment in time, and the prolonged lying on the ground may turn a non-fatal fall to a fatal one.

Numerous literature proposed fall detection machine using vision, IMUs, and radio frequency. However, none of these fulfills the requirement of being privacy-protected, device-free, training-free, and low false-alarm. As a human fall will cause a huge impact on the floor, one way to recognize a human fall is to analyze the floor vibration, but there are only a few works can be mentioned. In [4], the authors

proposed an automatic fall detection machine by deploying an accelerometer on the floor. However, this system requires the assistance of an acoustic microphone at the same time. It only evaluates a mimicking human doll falls forward, and it is a data-based system which fails with other test samples.

To implement a reliable vibration-based fall detection system, we need to address the following challenges: i) The floor vibration profile induced by many other objects fall from a certain height is similar to human fall. How can we distinguish a risky fall event from others? ii) It is impossible to let the elders fall on the floor to train a classification model as most systems do. Is there any way to realize a training-free fall detection system by building a general template for all the elders? iii) The demanding recognition task also results in a high false alarm rate, making the system user-unfriendly. What could we do to reduce the false alarm rate without the intentional intervene by users?

In this paper, we first introduce two typical falling mode: trip and slip. By comparing the waveform and spectrum of vibration signals induced by different events, we find out that a floor vibration profile of human fall has two special *transition states*. We characterize the fall-induced vibration signals based on the Discrete Wavelet Transform (DWT) which provides a good trade-off for signals between time and frequency domain and enables a good measurement of a fall event. Then, we are able to recognize the testing fall samples precisely by training a Hidden Markov Model (HMM) as a template with a small number of training samples (e.g., 50 fall samples in our baseline evaluation).

However, some of the vibration events have a similar pattern of a human fall after applying DWT to the vibration signals and thus cause a false alarm. In order to reduce the false alarm rate, we propose a reconfirmation mechanism in the assistance of EoA positioning. EoA, referred to as Energy-of-Arrival, is an indoor positioning algorithm, which calculates the ratio of received signals energy between each pair of sensors. In contrast to the time difference of arrival (TDoA) mechanism which requires high temporal resolution provided by a high sampling rate, EoA requires no time information recorded by sensors but only the energy of arrival. This makes the EoA mechanism has a better performance especially when the sampling rate is low and the time estimation error is high.

We implement G-Fall as a real-time fall detection system on a Raspberry Pi with three geophones. Experiment results show that G-Fall can characterize the fall event effectively and

---

*These authors contribute equally to this work.

achieve 95.74% of recognition precision with false alarm rate at 5.30%. Furthermore, the false alarm rate is reduced to nearly 0% with the assistance of the EoA reconfirmation mechanism,

In summary, the main contribution of this paper lies in the following aspects.

- To the best of our knowledge, G-Fall is the first work to realize a privacy-protected, device-free, training-free, and low false-alarm fall detection machine with geophone sensors.
- We propose a novel mechanism based on Energy-of-Arrival (EoA), which enables the system to achieve fine-grained indoor positioning without high sample frequency. The false alarm rate is reduced from 5.30% to nearly 0% using EoA.
- We design and implement the real-time automatic fall detection machine leveraging the floor vibration. Extensive experiments in a typical indoor scenario demonstrate its feasibility of fall detection, achieving a high precision of 95.74%.

The remainder of this paper is organized as follows. We first introduce the related work in Section II. Then in Section III, we analyze the vibration waveform and spectrum, followed by the description of design goals and three main modules of G-Fall in Section IV. We illustrate our methodology in Section V. Section VI explains the implementation detail and provides evaluation results of G-Fall. Finally, the discussion and conclusion are given in Section VII and Section VIII, respectively.

II. RELATED WORK

Existing fall detection systems: Over the past decade, extensive fall detection systems have been proposed. They can be categorized as following four classes: vision based, IMUs based, wireless radio based and ambient device based.

Vision-based fall detection systems [5]–[7] can detect a falls event effectively after analyzing a series of images recorded by high-resolution cameras using complex activity recognition algorithms such as deep learning. Nonetheless, it lacks privacy concern, for example, it is impossible to employ a camera in the bathroom to detect a slip event. What's more, the vision-based systems fail to work under dark environment and non-line-of-sight condition.

Numerous literature utilized the embedded Inertial Measurement Units (IMUs) in the wearable device to detect a fall [8]–[10]. They can recognize a fall event by monitoring and analyzing the reading changes of accelerometer, gyroscope and inclinometer. However, it is obtrusive and user-unfriendly to carry a device, and the elders always forget to wear the smartwatch.

Wireless radio is a good choice to realize a device-free fall detection systems [11]–[13]. They require no on-body device and bring no privacy issues, which makes the wireless radio the most promising and charming research trend to realize device-free fall detection systems. Nevertheless, the high false alarm rate has been criticized for a long time, and the multipath
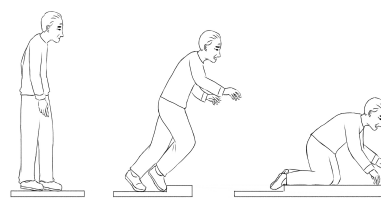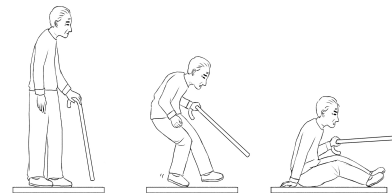

Fig. 1. Process of a trip

Fig. 2. Process of a slip

effect of wireless signals make it difficult to work in a dynamic home environment.

As for ambient device based, audio [14] and floor vibration [4] are used to characterize a human fall. The audio-based systems need to sense the sound of everything in the surroundings and have poor resistance to noise, leading to a large proportion of false alarm. There are also many challenges in realizing a fall detection system using floor vibration. However, the vibration signals propagating through the floor suffer almost zero multipath effect. And the signals can retain well even in a dynamic and complex environment [15]. In this paper, we propose a device-free, training-free, and positioning-assisted fall detection system with only vibration sensors, which can accurately distinguish a human fall from daily living activities or other objects that fall from a certain height.

Device-free indoor positioning: Another important technique related to G-Fall is device-free indoor positioning. Occupants can be located with ambient sensors instead of carrying wearable devices. RF signal, acoustic, Ultra-wideband (UWB), cameras and so on are used for indoor positioning. To reduce the multipath effect of RF signals and acoustic, Floc [15] suggested a vibration positioning methods with a SWIM algorithm to detect the footsteps. [16] utilized the wavelet transform and TDoA to localize the vibration of footsteps. Pan et al. designed a hardware system called BOES [17] to collect the footstep vibration and track the occupants. However, these works required a high sampling rate to capture the precise value of TDoA. We propose an EoA mechanism to localize footsteps with the energy ratio between geophones in low frequency. We successfully reduce the false alarm rate to nearly 0% with EoA.

Vibration-based smart sensing: There are many interesting vibration-based smart sensing system proposed in recent years. FootprintID [18] utilized footsteps vibration to identify occupants with an iterative transductive learning algorithm. Pan et al. [19] presented a method to monitor multiple occupant traffic by sensing the ambient structural vibration. The system achieves occupant traffic monitoring by acquiring
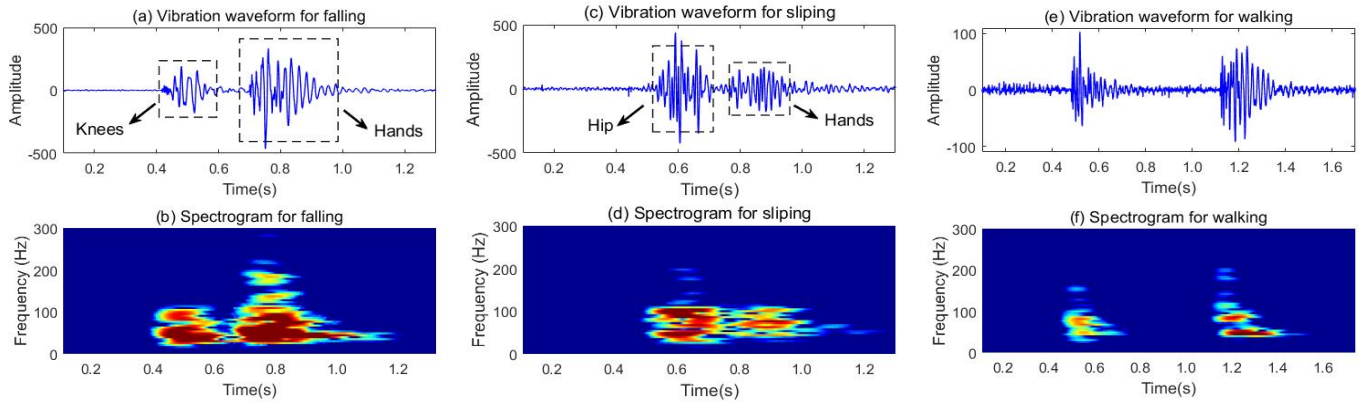
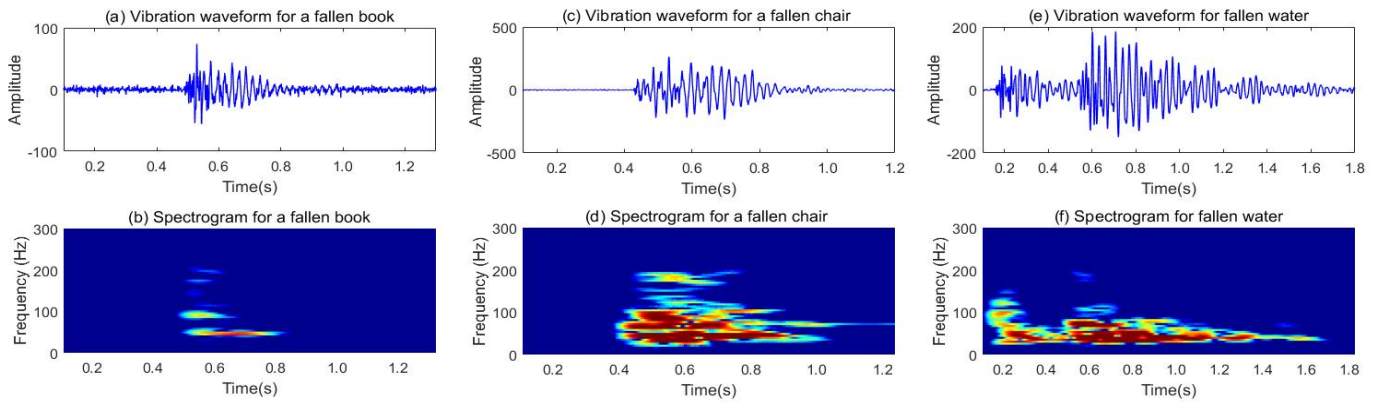Fig. 3. Waveforms and spectrograms for body-induced vibration signals

Fig. 4. Waveforms and spectrograms for object-induced vibration signals

signals from structural vibration sensors and analyzing their features. D Bales et al. [20] used footsteps vibration to classify gender. [21] [22] used geophones to detect vibration to monitor heartbeats when people are lying on the bed. There are some works [23]–[26] using vibration to localize the finger tapping to realize text input.

III. PRELIMINARY STUDY

The key reasons for a fall event for the elderly are *i)* physical lesions incur the uncoordinated walking or faint. *ii)* losing balance on a slippery floor such as in a bathroom. *iii)* falling over the obstacles due to poor vision. Thus, we generally classified the falling mode as *trip* and *slip*, as shown in Fig. 1 and Fig. 2. During the process of a trip, the knees usually hit the ground first, and then the hands are supported on the ground. In contrast, slip leads to the first landing of the hip and followed by the support of hands or elbows.

In a typical house layout, there are many vibration sources such as human's walk, falling books, chairs or bottles. Therefore, in this Section, we first study the waveform and spectrum of the objects mentioned above.

Experimental Setup: We set up the pilot test in a $6m \times 8m$ laboratory. Three geophones are respectively placed at three corners on the anti-static floor covering an area of $3m \times 4.8m$

as shown in Fig. 9. This area can be estimated as a typical area of living room or bathroom. The sampling rate of G-Fall is set to be $1190Hz$. For body-induced vibration, as shown in Fig. 9, we collect the signal of trips and slips on the red circle area and the condescending footsteps along the track with an interval of $60cm$. For object-induced vibration, we record the falling of a bottle of $400ml$ water, a 400-page book, a $2.5kg$ chair. The bottle and book fall from a 50cm high desk.

Body-induced vibration: The waveform and spectrum of trip and slip are shown in Fig. 3(a)-(d), where high-energy frequency components are colored in red. During a trip, the human body has a forward trend. In phase one, the knee is centered on the foot and uses the length of the calf as the radius to make the circular motion. But in phase two, the remaining parts of the body make the circular motion centered on landed knees, which results in a more considerable angular velocity when the hands are landing. This process is represented as a waveform of relatively low amplitude followed by a higher one in the time domain. As for a slip, in reverse, most of the falling force is neutralized when the hip is landing. The support hands suffer smaller force then. There is a slight difference between a trip and slip, but they both comprise two obvious *transition states* on account that different part of the body contacts the

floor in sequence. And compared to that of a footstep in Fig. 4(e)-(f), falls have a longer duration and higher energy.

Object-induced vibration: When it comes to object-induced vibration event, from Fig. 3(a) and (c), the waveforms for the book and chair seem to be more stable, unlike that of a fall which has two obvious *transition states*. This is because the rebound height of the chair is relatively low and even no for a book. As for the bottle, after the rebound, it tends to roll on the floor, resulting in a longer vibration signal.

Summary of observation: From the analysis above, we have two observations: *i)* the vibration signals of a fall event comprise two unique *transition states*, which is distinct from other events; *ii)* a fall event, compared to a walk event which is the main vibration source in daily life, has larger amplitude and longer duration. These two observations provide us with a hint to extract energy features and leverage the Hidden Markov Model (HMM) to identify a human fall. (see more details in Section V).

IV. SYSTEM OVERVIEW

A. Design Goals

G-Fall is designed to meet the following goals, which are the basic properties if we want to put G-Fall into practical use.

1) Training-free: Traditional fall detection systems are data-based and adopt machine learning algorithms that require the users to train their own falling models in advanced. However, it is impossible for these data-based fall detection machines to collect the fall data from the elders. Therefore, G-Fall needs to find a way to make sure it is a training-free system for specific users.

2) High recognition accuracy: Timely fall detection and warning is about saving lives, and ideally, we do not want to miss the detection of each human fall event. Thus we have to make sure the system provides a high recognition accuracy for human fall.

3) Zero false alarm: It will be user-unfriendly and obtrusive for the elder if they need to clear the alarm in person when a false alarm happens. People will take hundreds of steps walk a day, and then tens of clear operation are needed if the false alarm rate is 10%. Thus, we have to find a suitable solution to reduce the false alarm to zero as much as possible.

B. System Overview

The system architecture of G-Fall comprises three major components in order to build a reliable system for automatic fall detection. The following is the description of these components.

1) Signals Detection: G-Fall employs three geophone sensors to convert the vibration signals into digitalized electrical signals. Then the signals are denoised using a 20Hz Butterworth high pass filter and segmented using an energy-based dual-threshold mechanism.

2) Fall Recognition: In the classification phase, G-Fall extracts the unique features through Discrete Wavelet Transform (DWT) based on the observation after the decomposition of a fall event in the preliminary study. Then, a Hidden Markov Model (HMM) is applied to complete a fall recognition.
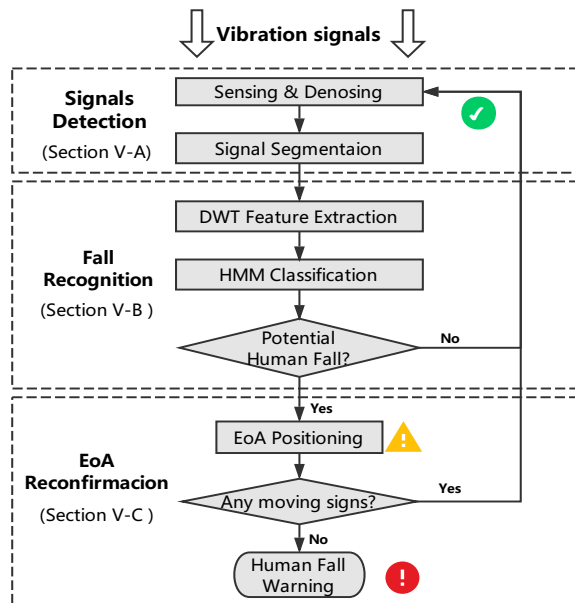

Fig. 5. System Overview of G-Fall

3) EoA Reconfirmation: In order to realize a zero false-alarm fall detection system, in G-Fall, we adopt a straightforward but efficient idea with the assistance of positioning. We come up with a novel positioning algorithm: Energy-of-Arrival (EoA), which achieves decimeter-scale positioning and reduces the false-alarm rate to nearly 0%.

Fig. 5 presents the work-flow of G-Fall. In the detection phase, the system is sensing for vibration signal that breaks the dual-threshold. When a vibration event is sensed, the signals will be denoised and segmented. Afterwards, G-Fall extracts the features of signals using DWT and matches the pattern with the pre-trained HMM template in the database to judge whether a potential human fall occurs. If so, the EoA reconfirmation module will be turned on, and the system will reconfirm the potential human fall with EoA mechanism by detecting the moving signs of a human. A warning message will be sent out for asking help ultimately if there are no signs of human movement in a certain time; otherwise, the system will regard the potential human fall as a false alarm and keep sensing again without warning.

V. METHODOLOGY

In this section, we illustrate the details of G-Fall in three major modules.

A. Signals Detection & Process

1) Sensing & Denosing: The geophone is designed as a device for converting ground mechanical vibration signal excited by an artificial source into an electrical one. Fig. 8 demonstrates the geophones we adopt, a cylinder whose external diameter is $25\ mm$ and the height is $30\ mm$. It

is sufficient to detect fall with one geophone sensor, but the EoA positioning algorithm we design requires at least three geophones. Fall-induced vibration signals are realized in low frequencies domain (less than $300\ Hz$), and we sample them using Raspberry Pi with a sampling frequency of $1190\ Hz$. We leverage a 20 Hz Butterworth high pass filter to remove the noise caused by the direct current component.

2) Segmentation: We adopt an energy-based dual-threshold scheme to catch a fall event [15]. The energy levels are calculated as the sum of the square of received signals in a sliding window. The lower threshold is $\mu+\sigma$, which is sensitive to break. And the higher one is $\mu + 3\sigma$. The μ and σ are the mean and standard deviation of signal energy, respectively. When the upper threshold is exceeded, the lower threshold will be considered as the start point of the detected signal. As for the endpoint, we set it at 0.8 s after the start point, as the duration of a fall is usually around it. Note that when a potential fall event is detected, the upper threshold will be reset for sensitive detection of a footstep in EoA. We deploy three sensors in G-Fall, but only one channel with the highest energy level will be segmented for feature extraction and input HMM.

B. Fall Event Classification

1) Feature extraction: We model the fall event by profiling the energy of each component in the frequency domain derived from Time-Frequency analysis tool—Short-Time Fourier Transform (STFT). However, in order to extract frequencies at multiple resolutions with respect to various time scales, the most relevant signal processing tool is discrete wavelet transform (DWT). Comparing to STFT, the advantages of DWT are [12]: *i)* DWT performs a nice tradeoff between time and frequency resolution, and it groups frequencies that differ by several orders of magnitude into a few levels so that it can characterize the whole fall event. *ii)* DWT reduces the size of the input sample so that the system can operate in real time. We calculate the energies for 8 levels using Daubechies wavelet in the order of 6 and extracts a 100-dimensional feature vector.

2) Recognition with HMM: Recall that the observation in Section 2, we can infer that a senior is probably falling when looking at the transition between two states. Hidden Markov Model (HMM) is a suitable method to establish a state transition model using time-dependent features. HMM has been successfully applied in several recognition applications such as speech [27], handwriting, and gesture [28] recognition. It is based on the assumption of a Markov chain: the state of the next moment is determined only by the current state, and does not depend on any state in the past. The probability from the current state to the next state is defined as *transition probability*, and the probability of obtaining each potential observed value based on the current state is called *emission probability*. Afterwards, an HMM can be established given an *initial state vector*. We get the final HMM model $\lambda = (A, B, \Pi)$ by using a small number of fall samples to train the three parameters: transition probability matrix A, emission probability matrix

B, and initial state vector Π. Given an *observation sequence*, i.e., the vibration signal, HMM can tell how likely it is to be a human fall.

Specifically, we estimate the mean vector and covariance matrix corresponding to each state and the transition probability with the well-known Baum-Welch Algorithm [29]. And we finally decide the number of states to be 7 by iterating through a different number of states and select the optimal one. Note that the states in HMM are abstract parameters that do not relate to the body state directly.

C. EoA Reconfirmation with Energy-of-Arrival (EoA)

1) Why EoA?: To eliminate the obtrusive false alarm, we propose a straightforward yet effective idea that we can reconfirm the existence of a risky fall event with the assistance of indoor positioning. When a risky fall event occurs, in an ordinary situation, the elderly lose their ability to make any further movement to a new location. Therefore, if a series of movement activities are captured using an indoor positioning algorithm after a potential fall event is detected, we can intuitively consider it as a false alarm and clear the warning automatically without the intervention of humans. This makes the system practical and user-friendly. Note that detecting any vibration signals is not a necessary hint to clear the alarm, because the fallen elder might stay conscious and struggle in situ causing vibration on the floor.

Previous works [15] [16] realized decimeter-scale indoor multilateration with three geophones using TDoA algorithm. Estimating accurate time difference is essential for good positioning performance when using TDoA [30], but this requires more complex hardware to provide high sample frequency and thus increase the computation overhead. Furthermore, the dispersion nature of floor vibration during propagation resulting in different frequency components of wave travel at different velocities [31] [32]. As a result, the estimated propagation velocity of vibration signal varies largely, making an unacceptable shift for located points when using TDoA.

Thus, we come up with a novel algorithm EoA, which can realize fine-grained positioning at a low sample rate without the estimation of the time difference and propagation velocity.

2) EoA Model and Principles: The key innovation of G-Fall lies in reducing false alarm rate to zero using Energy-of-Arrival (EoA) mechanism with low sample frequency. The illustration of a multilateration using three geophones is shown in Fig. 6.

More specifically, during the horizontal propagation of a footstep-induced vibration, the signals will suffer attenuation, and the model can be described as [33]:

$$Amp(d) = Amp_0 e^{-\alpha \times d} \tag{1}$$

where Amp_0 is the initial amplitude, d is the propagation distance, and α is the attenuation coefficient depend on the propagation media.

Now, given the amplitudes of arrival for three geophones regarding to a certain distance d_1, d_2, d_3 respectively to be
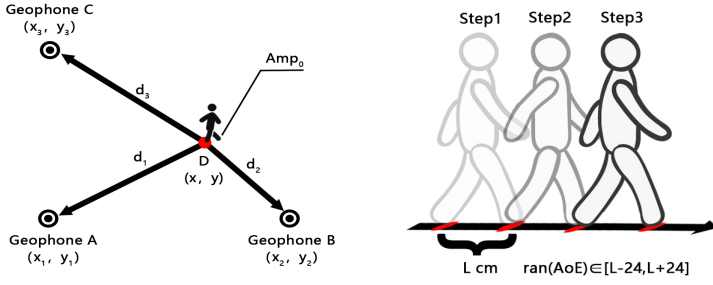
Fig. 6. An illustration of EoA positioning in G-Fall.

Fig. 7. An illustration of continuous walk for three steps.

Fig. 8. A sample prototype of G-Fall

$$A(d_1) = Amp_0 e^{-\alpha \times d_1}$$
$$B(d_2) = Amp_0 e^{-\alpha \times d_2} \quad (2)$$
$$C(d_3) = Amp_0 e^{-\alpha \times d_3}$$

We then can calculate the energy of arrival for the attenuated vibration signal from the reading of three geophone sensors. By dividing any pair of energy recorded by geophone, the initial amplitude of signals will be canceled out:

$$E_{AB} = \frac{A^2(d_1)}{B^2(d_2)} = \left(\frac{Amp_0 e^{-\alpha \times d_1}}{Amp_0 e^{-\alpha \times d_2}}\right)^2 = e^{-2\alpha \times (d_1 - d_2)} \quad (3)$$

where E_{AB} is the ratio of energy of arrival from geophone A to that from geophone B.

Given signals from a known coordinate point, we can calculate E_{AB}, d_1 and d_2. Then, we can estimate an attenuation coefficient α of the floor from Equation (3). Afterwards, given any vibration signals generated from an unknown location. We have the following relationship based on the energy of arrival:

$$d_1 - d_2 = \frac{\ln E_{AB}}{-2\alpha} = c_1 \quad (4)$$

$$d_1 - d_3 = \frac{\ln E_{AC}}{-2\alpha} = c_2 \quad (5)$$

where c_1 and c_2 are constant.

From Equation (4), we find that the unknown point $D(x,y)$ is a moving point that the difference of the distances from two fixed points is a constant, which means the trajectory of $D(x,y)$ is one side of a hyperbola. And the intersection of another hyperbola is the estimation of vibration source.

3) Detection of Moving Signs: In Fig. 7, we depict a continuous walk of three steps with stride length of Lcm. The stride length vary from $40cm$ to $80cm$ for the elders aged over 60 [34]. Given the estimation error of EoA is below 24cm (see Fig. 13), the estimated coordinate of fall position is $P_0(n_0, m_0)$ and that of next three steps is $P_1(n_1, m_1)$, $P_2(n_2, m_2)$, $P_3(n_3, m_3)$ respectively, we acquire a lowest threshold THR to judge a movement:

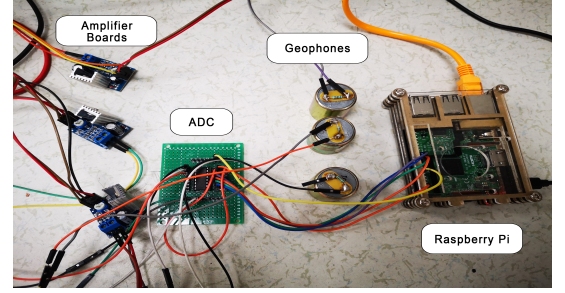$$THR = \sum_{i=1}^{3} \sqrt{(n_i - n_0)^2 + (m_i - m_0)^2} \quad (6)$$

The threshold will be hard to reach if a potential fall event is detected and the fallen elder struggles in situ. G-Fall regards the potential fall event as a real and fatal one and sends the warning message if the threshold is not exceeded in a preset time. But once it is overpassed, we consider a further movement of human occurs, and the potential fall event is a false alarm.

VI. EVALUATION

This section will present the implementation and experimental settings of G-Fall first, followed by the results for recognizing a fall event under different setting and verifying the effectiveness of EoA mechanism.

A. Experimental setting

Implementation:

We implement a prototype (see Fig. 8) with a Raspberry Pi controller and an Analog to Digital Converter (ADC). Three geophones with amplifiers were used to collect vibration signals. We set amplifiers as 100X and sampling rate as 1190 Hz. To fix the sampling rate, we used BCM2835 Library with C. In order to realize a real-time system, we transmitted signals to a conventional desktop computer by a PL2303 USB To Transistor-transistor logic (TTL) Converter Adapter Module via WiringPi Library with C. The data is then analyzed in MATLAB platform.

Experimental setup:

The experiment environment is a typical $6m \times 8m$ lab with the anti-static floor. Three geophones cover an area of $3m \times 4.8m$ as shown in Fig. 9. To evaluate our systems, we recruited 12 participants (2 of them are female) whose height, weight, and age are in the range of 156cm–182cm, 48kg–68kg, and 19–29 respectively. And the height-weight-age table of the participants is listed in Table I.

All the data are collected and saved for off-line analysis with G-Fall system running in real time. Each experiment is repeated for ten times to get the average results. The participants are asked to perform the actions described in Table II, each for 25 times, resulting in 5400 responses $((10 \ actions + 2 \ walks \times 4 \ steps) \times 25 \ times \times 12 \ subjects)$. Note that the participants are asked to perform trips and slips depicted in Fig. 1 and 2 as real as possible. And they are given a 2-minute warm-up period to practice the required actions.
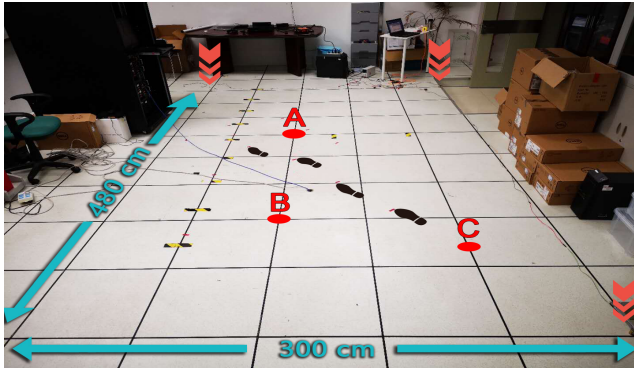
Fig. 9. A lab with anti-static floor. The red arrows point at the geophones.

TABLE I
The height-weight-age table of the participants

No.	H(cm)	W(kg)	Age	No.	H(cm)	W(kg)	Age
1	178	58	19	7	168	58	21
2	179	57	20	8	181	68	22
3	170	60	26	9	168	58	21
4	177	66	27	10	156	48	20
5	165	61	29	11	168	52	20
6	168	55	20	12	182	59	21

As for objects, we perform the falling of a bottle of 400ml water, a 400 pages book, and a 2.5kg chair, each for 25 times respectively, generating 75 responses ($25\ times \times 3\ objects$). Note that all the participants are required to wear protective gears when falling, and a cushion is also used when performing slip for protecting hip bone. The whole process of falling brings no harm to the subjects. And all the experiments involved human subjects have been approved by the Institutional Review Board in our university.

Metrics: We introduce two metrics to analyze the performance of G-Fall, namely, recognition precision ($Precesion$) and false-alarm rate (P_{fls}). The definitions are shown as follows. Note that other events refer to all the non-human fall events.

$$Precision = \frac{\#\ of\ truly\ detected\ fall}{\#\ of\ human\ fall} \quad (7)$$

$$P_{fls} = \frac{\#\ of\ wrongly\ detected\ fall}{\#\ of\ other\ events} \quad (8)$$

B. Recognition accuracy

1) Baseline Performance: We first perform a baseline test for recognizing fall event with only one person in the training set. Specifically, the 50 fall samples (25 trips and 25 slips) in location A of each participant are used to train the HMM in turn before testing with the rest of the samples. The detailed statistics are listed in Table III. In total, with only one person in the training set, 495.45 out of 550 human falls are detected correctly, yielding a precision of 90.08% with the false-alarm rate at 12.30% on average. We mark this as the baseline performance of G-Fall.

TABLE II
Description of actions for the data collection

Standard Fall	Loc.	||	Other Actions	Loc.
Trip forward	A	||	Sit	A
Trip forward	B	||	Mark time Heavily	A
Trip forward	C	||	Fall forward from a chair	A
Slip backward	A	||	Trip forward-Hold on a chair	A
Slip backward	B	||	Walk normally along the track	Track
Slip backward	C	||	Walk heavily along the track	Track

TABLE III
Baseline performance of G-Fall with one person in the training set

Event ＼ Class. As	Human Fall	Others	Total	Accuracy
Human Fall	495.45	54.55	550	90.08%
Sit	22.68	277.32	300	92.44%
Mark Time	22.68	277.32	300	78.65%
Normal Walk	54.81	1145.19	1200	95.43%
Heavy Walk	227.41	972.59	1200	81.05%
Objects	6.75	68.25	75	91.00%

We notice that the majority of false alarms is contributed by the "heavy actions" like marking time and walking heavily. However, the other results show that our system is relatively robust that will not take the normal daily activities as human fall easily. The uniqueness of a human fall is mainly because of the *transition state* mentioned in Section III. And the process of human fall that we decompose has two parts of body contact with the floor, which can also be considered as two objects fall successively during a short time. This happens uncommonly and makes the human fall distinguishable from other events. Furthermore, in Table IV, comparing to other machine learning algorithms, HMM does present better performance when applying DWT which extracts the time-dependent features from the vibration profile of the human fall.

2) Impact of training set size: Since G-Fall characterizes the general fall event through a training-free HMM template, we need to train the template as best as possible before practical use. Intuitively, the recognition performance of our system can be improved by enlarging the training set size. To verify this hypothesis, we evaluate the performance by increasing the number of people in training set from 1 to 7, and the results are given in Fig. 11. We can see that the recognition precision rises upward monotonically from 90.08% to 95.74% with the increase in the number of training people. And the false-alarm rate drop at the same time to the minimum of 5.30% with a seven-person-trained HMM. This indicates that G-Fall does have a better performance if we diverse the initial training sets with more people's fall samples.

3) Impact of different locations: As a training-free fall detection system, G-Fall should function properly and recognize the human fall event at any location even though it depends on a template trained by the samples collected from a specific location. For example, if we build a template using the fall samples collected at location A, the system should recognize a fall at location B or C. To validate this hypothesis, we trained the HMM in turn with 25 trips and 25 slips samples of each subject at location A, then test it using the remaining fall
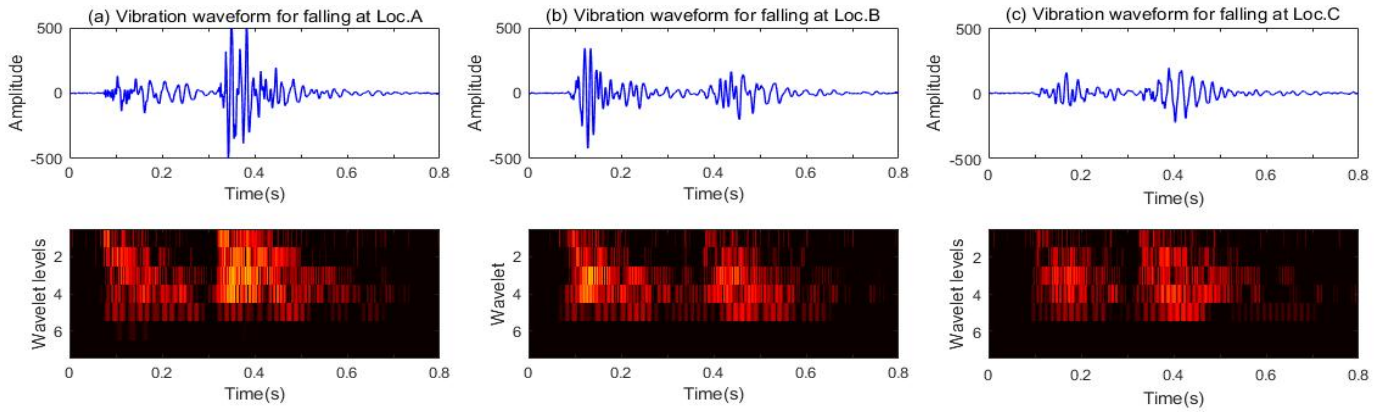
Fig. 10. Discrete wavelet transform (DWT) of time-series for human fall at different location regarding to the same geophone.
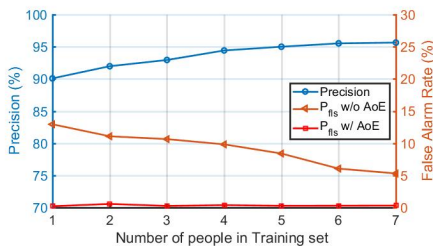

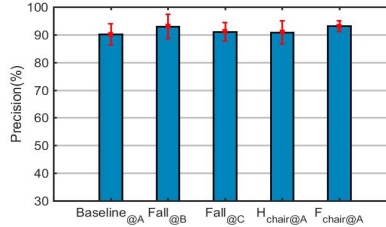Fig. 11. Impact of training set size for G-Fall

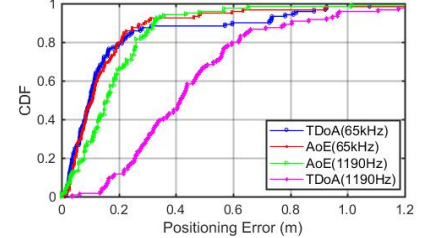Fig. 12. Impact of different location and non-standard fall for G-Fall

Fig. 13. The positioning error of TDoA and EoA with sample rate at 65kHz and 1190Hz

TABLE IV
Comparison of different classifier with one person in the training set

Items	HMM [29]	KNN [35]	SVM [36]	BPNN [37]
$Precision$	90.08%	83.21%	79.73%	82.08%
P_{fls}	12.30%	17.34%	12.55%	15.70%

samples collected at B and C. The results are shown in Fig. 12, where the precision suffers no degradation when testing with the samples from other locations. This verifies that G-Fall can recognize human fall at anywhere even if we train the template with the human fall samples collected from only one specific location.

Fig. 10(a)-(c) plot the vibration waveforms collected from different falling location and its corresponding DWT. From these figures, we observe that the DWT features that G-Fall extract follows similar pattern even though the vibration waveforms vary from each other.

4) Impact of non-standard fall: We select two typical fall modes: trip and slip as a standard to represent the majority of the fall event. However, there is a great variety of posture when users fall in practical. To study the impact when people perform non-standard falls, we ask 12 of our participants to fall from a $45cm$ height chair ($F_{chair@A}$) and fall with their hands held on a chair at last($H_{chair@A}$), each for 25 times. We train the HMM with only one participant's 50 fall samples (25 trips and 25 slips) and test with the non-standard fall samples. In Fig. 12, we can see that there is also no impact on the system performance when testing with non-standard fall. The result

indicates that G-Fall can recognize a certain falling pattern with HMM as classifier even when some posture variation of fall occurs. We think this is because the signals of floor vibration suffer less influence from complex human motions comparing to those fall detection systems which capture the human motions using accelerometer or gyroscope.

C. Effectiveness of Energy-of-Arrival

1) Accuracy of EoA: To realize positioning with TDoA and EoA, we first use three known points to estimate the wave velocity v_0 and the attenuation coefficient α, yielding v_0 of $220m/s$ and α of 0.2961. Then, we select the other 6 points as ground truth, estimating the coordinate for 20 times each using TDoA and EoA respectively. Fig. 13 shows the results of positioning performance for different sample rate and methods. EoA achieves nearly the same performance as TDoA with high sample rate at 65kHz, and there is an 80% possibility where the positioning error goes below 20cm. However, EoA outperforms TDoA when the sample rate drops to 1190Hz.

This is because the estimation of time difference become inaccurate under the situation of low sample rate, leading to a considerable shift from the ground truth, while the estimation of energy requiring low temporal resolution and suffer no obvious degradation under the same situation. What's more, the TDoA based positioning system using geophones is based on the assumption that the wave propagates velocity is stable. However, in fact, during propagation, the velocity varies a lot in a different direction because of the dispersion nature [31] [32]. Therefore, the inaccurate estimation of time difference

has a more significant impact on the positioning accuracy comparing to EoA whose assumption is that the attenuation coefficient of a specific media will not change.

2) After Reconfirmation with EoA : When a false alarm occurs, we assume that the elders will keep walking to clear the unsent alarm. Hence, we use the continuous four-step samples mentioned in the experimental setup to test the EoA reconfirmation module of G-Fall. So we can see from Fig. 11, when the EoA reconfirmation is turn on, the false alarm rate declined sharply to almost zero. However, indeed, the false alarm might still occur in some special case, but the results do verify the effectiveness of the EoA mechanism for reducing the false alarm rate.

VII. Conclusion

In this paper, we propose G-Fall, a positioning-assisted, zero false-alarm, device-free and training-free automatic fall detection system for single-resided elders. G-Fall deploys three geophones on the corners respectively to receive the floor vibration signals. We analyze the floor vibration induced by the human fall and extract time-dependent features to distinguish a human fall from other events with Hidden Markov Model. We prototype G-Fall with Raspberry Pi, which can recognize a fall event in real time with a user interface in MATLAB platform. The evaluation results demonstrate that G-Fall has a high potential to put into practical use.

Acknowledgment

References

[1] United Nations, Department of Economic and Social Affairs, Population Division (2017). World Population Ageing 2017 - Highlights (ST/ESA/SER.A/397).

[2] World Health Organization, "WHO Global Report on Falls Prevention in Older Age", World Health Organization, 2008.

[3] S. R. Lord, C. Sherrington, and H. B. Menz, "Falls in Older People: Risk Factors and Strategies for Prevention", Cambridge University Press, 2001.

[4] Dima Litvak Israel Gannot and Yaniv Zigel, "Detection of Falls at Home using Floor Vibrations and Sound", IEEE 25th Convention of Electrical and Electronics Engineers in Israel, pp. 514-518, 2008.

[5] E. E. Stone, M. Skubic, "Fall Detection in Homes of Older Adults using the Microsoft Kinect" IEEE J. Biomed. Health Inf. vol. 19, no. 1, pp. 290-301, 2015.

[6] G. Mastorakis, D. Makris, "Fall Detection System using Kinects Infrared Sensor", Journal of Real-Time Image Processing, vol. 9, no. 4, pp. 635-646, 2014.

[7] C. Krupitzer et al, "Hips Do Lie! A Position-Aware Mobile Fall Detection System", In Proc. IEEE Percom, 2018.

[8] Kau L.J, Chen C.S, "A Smart Phone-based Pocket Fall Accident Detection, Positioning, and Rescue System", IEEE J. Biomed. Health Inf., vol. 19, no. 4, pp. 44-56, 2015

[9] J. Wang et al, "An Enhanced Fall Detection System for Elderly Person Monitoring using Consumer Home Networks", Consumer Electronics IEEE Transactions, vol. 60, no. 1, pp. 23-29, 2014.

[10] P. Pierleoni A. Belli L. Palma M. Pellegrini L. Pernini S. Valenti, "A High Reliability Wearable Device for Elderly Fall Detection", IEEE Sensors Journal, vol. 15, no. 8, pp. 4544-4553, 2015.

[11] Y. Wang, K. Wu, and L. M. Ni, "Wifall: Device-free Fall Detection by Wireless Networks", IEEE Transactions on Mobile Computing, vol. 16, no. 2, pp. 581-594, 2017.

[12] W. Wang, A. X. Liu, M. Shahzad, K. Ling, and S. Lu, "Understanding and Modeling of Wifi Signal based Human Activity Recognition", In Proc. ACM MobiCom, pp. 65-76, 2015

[13] F. Adib, Z. Kabelac, and D. Katabi, "Multi-person Localization via RF Body Reflections", In Proc. 12th USENIX Conf. Netw. Syst. Des. Implementation, pp. 279-292, 2015.

[14] Y. Li, K. Ho, and M. Popescu, "A Microphone Array System for Automatic Fall Detection", IEEE Transactions on Biomedical Engineering, vol. 59, no. 5, pp. 12911301, 2012.

[15] W. Chen, M. Guan, L. Wang, R. Ruby, and K. Wu, "FLoc: Device-free Passive Indoor Localization in Complex Environments", In Proc. IEEE ICC, pp. 1-6, 2017.

[16] M. Mirshekari, S. Pan, P. Zhang, and H. Y Noh, "Characterizing Wave Propagation to Improve Indoor Step-level Person Localization using Floor Vibration", Sensors and Smart Structures Technologies for Civil, Mechanical, and Aerospace Systems, vol. 9803, p. 980305, 2016.

[17] S. Pan et al, "Boes: Building Occupancy Estimation System Using Sparse Ambient Vibration Monitoring", Sensors and Smart Structures Technologies for Civil, Mechanical, and Aerospace Systems, vol. 9061, p. 906110, 2014.

[18] S. Pan et al, "FootprintID: Indoor Pedestrian Identification through Ambient Structural Vibration Sensing." In Proc. ACM Ubicomp, 2017.

[19] S. Pan, M. Mishakeri, P. Zhang and H. Noh, "Occupant Traffic Estimation through Structural Vibration Sensing." SPIE Smart Structures and Materials+ Nondestructive Evaluation and Health Monitoring, pp. 980306-980306, 2016.

[20] D Bales, P Tarazaga, M Kasarda, and D Batra, "Gender Classification using Under Floor Vibration Measurements." Springer Dynamics of Coupled Structures, vol. 4, pp: 377-383, 2016.

[21] Z. Jia, A. Bonde, S. Li, C. Xu, J. Wang, Y. Zhang, R. E. Howard, and P. Zhang, "Monitoring a Persons Heart Rate and Respiratory Rate on a Shared Bed Using Geophones" In Proc. ACM Sensys, 2017.

[22] Z. Jia et al, "HB-Phone: A Bed-Mounted Geophone-Based Heartbeat Monitoring System" In Proc. ACM/IEEE IPSN, pp. 1-12, 2016.

[23] S. Pan, C. Ramirez, M. Mirshekari, J. Fagert, A. Chung, C. Hu, J. Shen, H. Noh, and P. Zhang, "SurfaceVibe: Vibration-Based Tap and Swipe Tracking on Ubiquitous Surfaces." In Proc. ACM/IEEE IPSN, 2017.

[24] J. Liu, Y. Chen, M. Gruteser, and Y. Wang, "VibSense: Sensing Touches on Ubiquitous Surfaces through Vibration" In Proc. IEEE SECON, 2017.

[25] W. Chen, Y. Lian, L. Wang, R. Ruby, W. Hu, and K. Wu, "Demo: Virtual Keyboard for Wearable Wristbands." In Proc. ACM SenSys, 2017.

[26] W. Chen, M. Guan, Y. Huang, L. Wang, R. Ruby, W. Hu, and K. Wu, "ViType: A Cost Efficient On-Body Typing System through Vibration", In Proc. IEEE SECON, 2018.

[27] L. R. Rabiner and B.-H. Juang, "Fundamentals of Speech Recognition", Prentice Hall, 1993.

[28] J. K. Aggarwal and S. R. Michael, "Human Activity Analysis: A review", ACM Computing Surveys, vol 43, no. 3, 2011.

[29] L. R. Welch, "Hidden Markov Models and the Baum-welch Algorithm", IEEE Information Theory Society Newsletter, vol 53, no. 4 pp. 1013, 2003.

[30] Coverley, P and Staszewski, W, "Impact Damage Location in Composite Structures using Optimized Sensor Triangulation Procedure", Smart materials and structures, vol. 12, no. 5, p. 795, 2003.

[31] Harley, J. B and Moura, J. M, "Sparse Recovery of the Multimodal and Dispersive Characteristics of Lamb waves", The Journal of the Acoustical Society of America, vol. 133, no. 5, pp. 2732-2745, 2013.

[32] Philippidis, T. and Aggelis, D., "Experimental Study of Wave Dispersion and Attenuation in Concrete", Ultrasonics, vol. 43, no. 7, pp. 584-595, 2005.

[33] A. Abdullah and E. F. Sichani, "Experimental Study of Attenuation Coefficient of Ultrasonic Waves in Concrete and Plaster", The International Journal of Advanced Manufacturing Technology, vol. 44, no. 5-6, pp. 421-427, 2009.

[34] Imms. F. J, Edholm. O. G, "Studies of Gait and Mobility in the Elderly", Age & Ageing, vol. 10, no. 3, pp 147-156, 1981.

[35] G. Guo et al, "KNN Model-Based Approach in Classification", Springer Berlin Heidelberg, pp. 986-996, 2003.

[36] C. C. Chang and C. J. Lin, "LIBSVM: a library for support vector machines", ACM Transactions on Intelligent Systems and Technology, vol. 2, p. 27, 2011.

[37] W. Jin, Z. J. Li, L. S. Wei, and H. Zhen. "The improvements of BP neural network learning algorithm", In Proc. IEEE WCCC-ICSP, vol. 3, pp. 1647-1649, 2000.